Am J Cancer Res 2024;14(12):5812-5825
www.ajcr.us /ISSN:2156-6976/ajcr0161725

Original Article

Combinatory actions of cytokines induce M2-like macrophages in anaplastic thyroid cancer

Takahito Kimura[1], Michael Kruhlak[2], Li Zhao[1], Eunmi Hwang[1], Laura Fozzatti[3], Sheue-Yann Cheng[1]

[1]Laboratory of Molecular Biology, National Cancer Institute, National Institutes of Health, Bethesda, MD 20892, USA; [2]Laboratory of Cancer Biology and Genetics, National Cancer Institute, National Institutes of Health, Bethesda, MD 20892, USA; [3]Departamento de Bioquímica Clínica, Facultad de Ciencias Químicas, Universidad Nacional de Córdoba, Córdoba 5000, Argentina

Received November 4, 2024; Accepted December 15, 2024; Epub December 15, 2024; Published December 30, 2024

Abstract: Anaplastic thyroid cancer (ATC) is a lethal endocrine malignancy. It has been shown that tumor-associated macrophages (TAMs) contribute to the aggressiveness of ATC. However, stimulatory factors that could facilitate the induction and infiltration of TAMs in the ATC tumor microenvironment (TME) are not fully elucidated. In this study, we used a human leukemia monocytic cell line (THP-1) to study the differentiation of THP-1 into M2-like macrophages (M2) by conditioned media (CM) derived from each of the three human ATC cells: 8505C, THJ-11T (11T), and THJ-16T (16T). The capacity of CM to induce M2 was in the order of 16T>8505C>11T cells as determined by the expression of M2 markers (CD163, CD204, and CCL13). Cytokine arrays and ELISA assays revealed five commonly enriched cytokines (IL-6, IL-8, MCP-1, TIMP-1, and TGF-β1) in the CM derived from each of the three ATC cells. These cytokines, individually, had weak activity, but together, they mimicked full CM activity in the induction of M2. Further, they collaboratively activated STAT3, ERK, and PI3K-AKT signaling to facilitate the induction of M2 as found in CM. Importantly, we found that the CM-induced M2 could secrete soluble growth factors to promote ATC cell proliferation as evidenced by the increased Ki-67, cMYC, and cyclin D1 protein levels. Our studies identified the major stimulatory cytokines which acted collaboratively to induce M2 in the TME. Importantly, the present studies indicate that when using inhibitors to target TAMs, combination therapies would be required for effective treatment of ATC.

Keywords: Anaplastic thyroid cancer, THP-1, monocyte differentiation, cytokines, tumor microenvironment, tumor-associated microphages

Introduction

Thyroid cancer is the most prevalent endocrine malignancy, with anaplastic thyroid cancer (ATC) being the most aggressive. ATC patients rarely survive beyond a year after diagnosis. One contributing factor to the aggressiveness of ATC could be the infiltrated tumor-associated macrophages (TAMs), which account for more than 50% of cell components in the tumor microenvironment (TME). TAMs have been reported to alter processes such as angiogenesis, tumor invasion, metastasis, and immunosuppression to promote aggressive tumorigenesis [1-4]. Based on these observations, we hypothesized that M2-like macrophages (M2) could be an underlying reason for the aggressiveness of ATC. However, how ATC tumor cells could induce M2 in the TME remains to be elucidated.

In the present studies, we aimed to identify soluble stimulatory factors secreted from ATC cells which could promote the differentiation of monocytes into M2. We used THP-1 cells, a human leukemia cell line, as a model to study the induction of M2 by the conditioned media (CM) derived from each of the three human ATC cells: 8505C, THJ-11T, or THJ-16 cells (designated as 11T and 16T hereafter, respectively). These three human ATC cell lines have different genetic lesions: 8505C cells have *BRAF*^{V600E} and *TP53* mutations, 11T cells harbor a *KRASG12T* mutation, and 16T cells have *TP53*, *RB*, and *PI3KCA* mutations [5]. We found that CM from each of the three ATC cells induced conversion of THP1 into M2, but the extent of conversion differed. We also identified the five major stimulatory cytokines (IL-6, IL-8, MCP-1, TIMP-1, and TGF-β1) enriched in the ATC CM to

https://doi.org/10.62347/QUWQ3794

induce M2. Importantly, we found that each of these cytokines alone did not induce M2, but acted collaboratively, promoting the differentiation of THP-1 into M2. The combinatory actions of these cytokines were through collective activation of the JAK/STAT, PI3K/AKT, and ERK pathways. We also found that CM-induced M2 could release growth factors to reciprocally promote proliferation of ATC tumor cells, in a feed-forward manner. The identification of multiple cytokines acting collaboratively to induce M2 suggested that combinatory therapies would be needed when considering targeting TAMs in ATC.

Materials and methods

Cell lines

The THP-1 cell line (human monocytes) was obtained from American Type Culture Collection (ATCC) and cultured in RPMI1640 medium as reported in [6]. Human ATC cell lines, 8505C, 11T, and 16T cells, were derived from human anaplastic thyroid cancers. 8505C was grown in DMEM, 11T and 16T were maintained in RPMI1640 as described previously [7, 8]. Each cell line was cultured in 5% CO_2 at 37°C in a humidified incubator.

Conditioned media

The ATC cell line, 8505C, was seeded at a density of 1×10^6 cells in DMEM supplemented with 10% fetal bovine serum (FBS) on 100 mm tissue culture plates. Similarly, 11T and 16T cells were seeded at 0.1×10^6 cells in RPMI-1640 containing 10% FBS. After an incubation period of 48 hours, the media was replaced with other media containing 5% FBS. Following an additional 48 hours, the conditioned media (CM) was collected and clarified by centrifugation at 300 g for 5 minutes. The CM was then utilized for treating THP-1 cells.

Induction of THP-1 to M2

THP-1 cells (1×10^6) were cultured for 24 hours in a 6-well plate with CM obtained from ATC cell lines. As a control, THP-1 cells were cultured in RPMI medium alone. Differentiation of THP-1 into M2 was assessed by the expression of M2 markers via mRNA and immunohistochemical analyses. Induction of M2 was also tested by treating THP-1 cells (1×10^6) with IL-6 (200 ng/ml), IL-8 (200 ng/ml), MCP-1 (10 ng/ml), TIMP-1 (100 ng/ml), and TGF-β1 (0.5 and 1.0 ng/ml). These cytokines were administered either individually or in combination, and their effects on differentiation were analyzed by the expression of M2 markers.

Real-time RT-PCR analysis

Total RNA extraction was performed using TRIzol. cDNA was generated using oligo dT primers and GoScript™ Reverse Transcriptase (Promega). PCR was performed using QuantStudio 3 (Applied Biosystems). The primers used are listed in Supplementary Table 1.

Western blot analysis

Western blot was performed as described previously [9]. Cell lysates were prepared by using cell extraction buffer, followed by centrifugation at 12,000 rpm for 30 minutes to collect the supernatant. After protein quantification, the lysates were then heated at 95°C for 5 minutes. Equal amounts of protein were loaded on Tris-glycine gels and transferred to 0.45 μm nitrocellulose membranes. Membranes were incubated with primary antibodies overnight at 4°C. After washing with TBS-T, the membranes were incubated with secondary antibodies for 1 hour at room temperature. Following additional washing with TBS-T, protein detection was performed using the ECL system. Band intensities were analysed by the ImageJ software (ImageJ 1.48v; Wayne Rasband, NIH). The antibodies against p-JAK2 (Tyr1007/1008), JAK2, p-STAT3 (Tyr705), STAT3, p-ERK (Tyr202/204), ERK, p-AKT (Ser473), AKT, p-mTOR (Ser2448), mTOR, p-p70 S6K (Thr389), β-actin, CD163, cMYC, Cyclin D1 were listed in Supplementary Table 2.

Immunohistochemical analysis

Cells were fixed in 10% neutral buffered formalin and embedded in paraffin. Sections were stained with hematoxylin and eosin. Immunohistochemistry (IHC) was performed using the previously described methods [10]. The antibodies CD163, CD206, Ki-67 were listed in Supplementary Table 2.

Preparation of green fluorescent protein (GFP)-labeled ATC cells

The three ATC cells (8505C, 11T, and 16T) were seeded at 2.5×10^4 per well in 6-well plate and

were transduced with lentivirus, which encodes the firefly luciferase (Luc2) cDNA fused with the enhanced green fluorescent protein (eGFP) cDNA, driven by FerH promoter (pFUGW-FerH-ffLuc2-eGFP) [11]. After expansion, cells were sorted to obtain cells enriched with GFP-8505C, GFP-11T, and GFP-16T cells for confocal imaging.

Live cell confocal imaging

The three ATC cell lines, 8505C-, 11T-, and 16T-GFP were co-cultured for 48 hours with THP-1 cells, which had been cultured for 24 hours in each respective CM. For control experiments, pure THP-1 cells were co-cultured with ATC-GFP cells. The number of GFP-positive cells was counted to assess the impact of ATC-GFP on cell growth. Extended field of view confocal images were acquired using a Nikon SoRa spinning disk microscope equipped with a 20× Apo LWDλS (N.A. 0.95) water immersion objective lens and Hamamatsu ORCA Fusion BT sCMOS camera. The tiled image series, covering the entire area of each well in a 4-well coverglass chamber (Ibidi cat#80427), were processed using the stitching algorithm in the Nikon Elements software (v. 5.4.1). GFP expressing cells were segmented using a modified Cellpose model [12] employed in an image analysis pipeline using Arivis Vision4D image analysis software (v. 4.1.2). The total number of GFP positive cells per well was counted for each cell type and treatment.

Analysis of expression of cytokines in thyroid cancer cells using The Cancer Genome Atlas database and GSE database

Gene expression of cytokines [*IL-6*, *CXCL8* (*IL-8*), CCL2 (*MCP-1*), *TIMP-1*, and *TGFB1*] in anaplastic thyroid carcinomas (ATCs) was analyzed using the Gene Expression Omnibus (GEO) database (https://www.ncbi.nlm.nih.gov/geo/). The dataset, GSE33630, included samples from 45 normal thyroids (Normal), 49 papillary thyroid carcinomas (PTC), and 11 anaplastic thyroid carcinomas (ATC). The dataset, GSE-65144, included samples from 13 normal thyroids (Normal) and 12 anaplastic thyroid carcinomas (ATC).

Statistical analysis

Statistical significance of differences between groups was analyzed by ANOVA or a two-tailed Student's t test. Statistical analysis was performed using GraphPad Prism. Data are presented as the mean ± SD. In all cases, p-values < 0.05 were considered statistically significant.

Results

Induction of differentiation of THP-1 cells into M2-like macrophages (M2)

CM from each of three ATC cell lines, 8505C, 11T, and 16T, was used to investigate the differentiation of THP-1 cells into M2 (**Figure 1A**). The M2 induction was characterized by evaluating mRNA and protein abundance of several M2 markers. The expression of M2 markers, *CD163*, *CD204*, and *CCL13*, was detected after culturing THP-1 in CM; but the capacity of CM inducing M2 effect was in the ranking order of 16T>8505C>11T cells (compare bar 4 with bars 2 and 3; **Figure 1B**).

We next analyzed the protein abundance of these M2 markers by IHC. The H & E staining are shown in **Figure 1C-I-a**, **1C-I-e**, **1C-I-i** and **1C-I-m** for THP-1 cells cultured in regular media or in CM derived from 8505C, 11T and 16T, respectively. Compared with THP-1 cultured in regular media (**Figure 1C-I-c** and **1C-I-d**, **1C-I-b** as IgG controls), the protein abundance of CD163 and CD206 cultured in CM derived from 8505C cells (**Figure 1C-I-g** and **1C-I-h**, **1C-I-f** as IgG controls), 11T cells (**Figure 1C-I-k** and **1C-I-l**, **1C-I-j** as IgG controls), and 16T cells (**Figure 1C-I-o** and **1C-I-p**, **1C-I-n** as IgG controls) was markedly elevated (**Figure 1C-II-a** and **1C-II-b**). These results indicated that the CM derived from ATC cell lines was enriched with stimulatory factors that induced the differentiation of THP-1 to M2.

Induction of THP-1 to M2 by combinatory cytokines enriched in CM derived from ATC cells

To identify the stimulatory cytokines in the ATC cells-derived CM that induced M2, we used a cytokine antibody array containing 80 human cytokines. Our analysis revealed strong signals from IL-6, IL-8, MCP-1, and TIMP-1 in the CM derived from 8505C cells (**Figure 2A-a**). In the CM derived from 11T, we detected signals from IL-8, TIMP-1, OPG, BDNF, MIP-1b, and GDNF (**Figure 2A-b**). In the CM derived from 16T cells, very strong signals of IL-6, IL-8, and TIMP-1 were detected (**Figure 2A-c**). Based on the find-

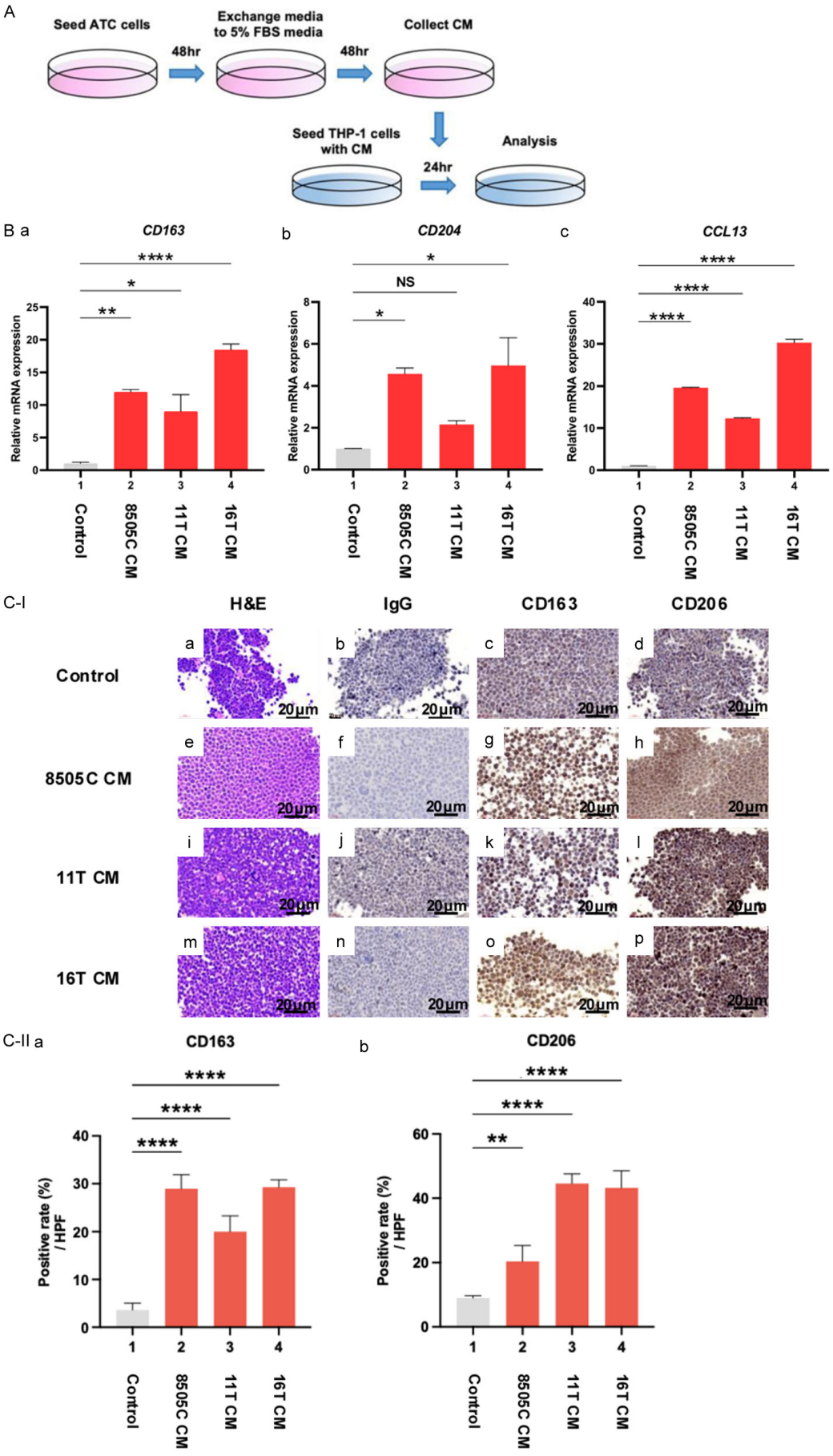
A
Seed ATC cells
48hr
Exchange media to 5% FBS media
48hr
Collect CM
Seed THP-1 cells with CM
24hr
Analysis
B a
CD163
b
CD204
c
CCL13
Relative mRNA expression
Control
8505C CM
11T CM
16T CM
NS
C-I
H&E
IgG
CD163
CD206
20μm
C-II a
CD163
b
CD206
Positive rate (%) / HPF

Figure 1. CM derived from ATC cells induces differentiation of THP-1 cells into M2. A. Schematic representation of the preparation of conditioned medium (CM) from ATC cells. THP-1 cells were treated with complete medium containing 5% FBS or CM derived from ATC cells for 24 hours. B. RT-qPCR analysis demonstrated a significant increase in the mRNA expression of M2 markers: *CD163* (a), *CD204* (b), and *CCL13* (c) in THP-1 cells treated with CM for 24 hours compared to those treated with control medium. C. Immunohistochemical (IHC) analysis of THP-1 cells treated with CM for 24 hours. Representative IHC images show staining with Hematoxylin & Eosin (H&E), IgG, CD163, and CD206 (C-I) (Magnification, bar scale =20 μm). Quantitative analyses of cells positively stained for CD163 and CD206 are presented (C-II). Data represent the mean ± SD (n=3). Significant differences are indicated by asterisks ($P < 0.05$ [*], $P < 0.01$ [**], $P < 0.001$ [***], and $P < 0.0001$ [****]). NS, not significant.

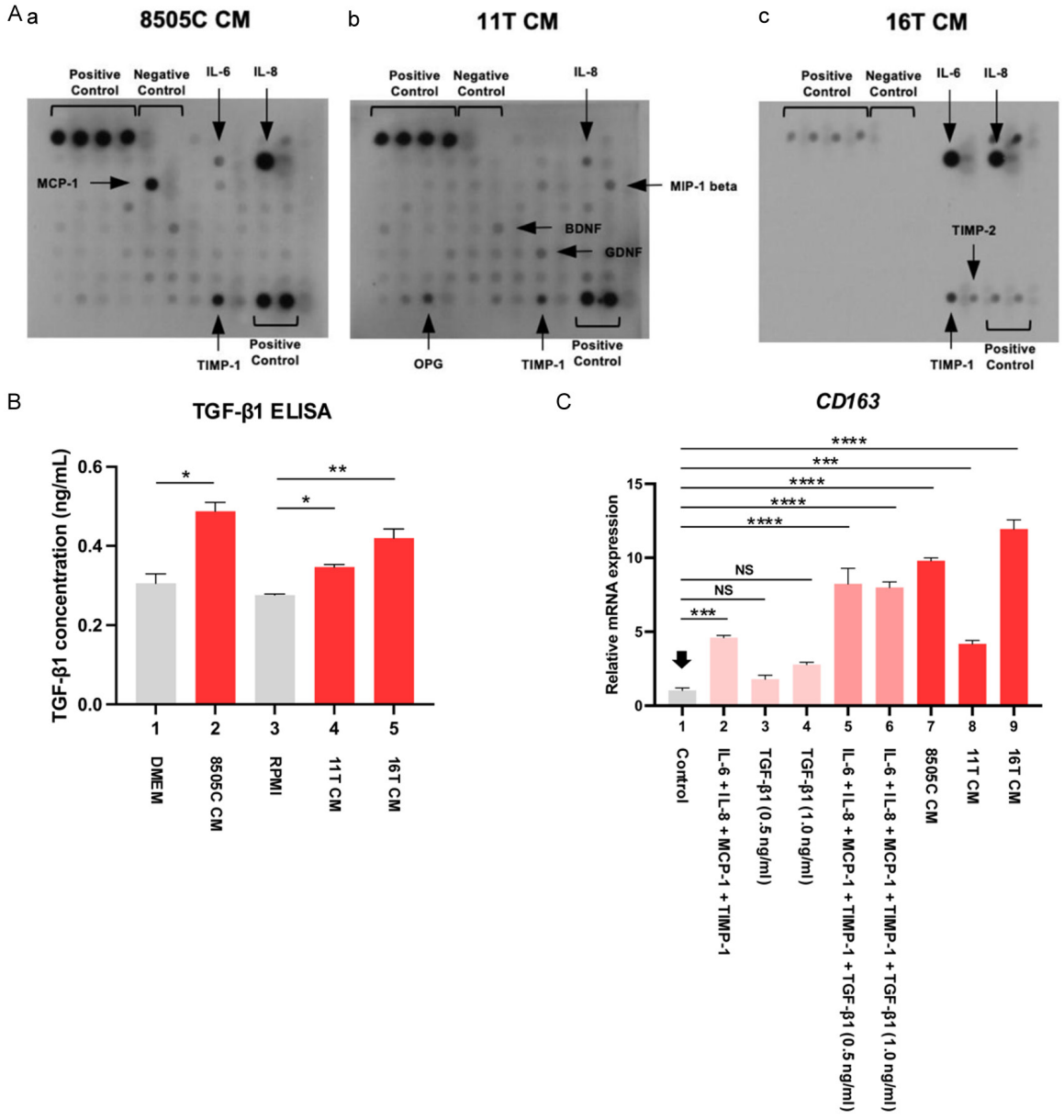

Figure 2. Identification and activity of stimulatory cytokines enriched in CM derived from ATC cells. A. Cytokine array profiling of CM from 8505C (a), 11T (b), and 16T (c). The cytokines detected above the background are indicated by arrows. B. Determination of concentration of TGF-β1 in CM derived from 8505C, 11T, and 16T by ELISA assays. Concentrations of TGF-β1 in 8505C, 11T, and 16T CM compared to normal culture medium (DMEM for 8505C CM; RPMI for 11T and 16T CM). C. RT-qPCR analysis of M2 marker, CD136, after treatment of THP-1 cells by a combination of cytokines as marked (IL-6; 200 ng/ml, IL-8; 200 ng/ml, MCP-1; 10 ng/ml, TIMP-1; 100 ng/ml and TGF-β1; 0.5 or 1.0 ng/ml). Data represent the mean ± SD (n=3). Significant differences are indicated by asterisks ($P < 0.05$ [*], $P < 0.01$ [**], $P < 0.001$ [***], and $P < 0.0001$ [****]). NS, not significant.

ings shown in **Figure 2B** and **2C**, we hypothesized that IL-6, IL-8, MCP-1, and TIMP-1 were major common cytokines that acted to differentiate THP-1 to M2.

Transforming growth factor-β1 (TGF-β1) is a pleiotropic cytokine, known to promote the differentiation of non-activating macrophages into M2 [13]. We therefore ascertained whether TGF-β1 was also present in the CM derived from 8505C, 11T, and 16T cells by using ELISA assays. Indeed, we found that TGF-β1 concentrations in 8505C CM were 1.6 times higher than the regular media (**Figure 2B**, compare bar 2 with bar 1) and in CM derived from 11T and 16T cells, they were 1.3- and 1.6-fold higher, respectively, than the regular media (**Figure 2B**, compare bars 4 and 5, with bar 3). **Figure 2B** shows that TGF-β1 concentrations were determined to be 0.5 ng/mL, 0.4 ng/mL, and 0.4 ng/mL in CM derived from 8505C, 11T, and 16T cells, respectively. Taken together, we have identified five cytokines (IL-6, IL-8, MCP-1, TIMP-1, and TGF-β1) that could contribute to the differentiation of THP-1 to M2.

We next tested each of these five cytokines for their activity to induce the differentiation of THP-1 into M2 by using M2 marker, CD163, as a read-out. The expression of CD163 was very low when THP-1 cells were treated with each of the five cytokines individually (IL-6, IL-8, MCP-1, TIMP-1, and TGF-β1) (Supplementary Figure 1). However, when THP-1 cells were treated with a combination of IL-6, IL-8, MCP-1, and TIMP-1 cytokines, a 4-fold induction was detected (compare bar 2 with bar 1, **Figure 2C**). When THP-1 cells were treated only with TGF-β1 at the same concentration found in CM (0.5 ng/mL or 1 ng/mL), no significant induction was detected (compare bars 3 and 4 with bar 1, **Figure 2C**). However, when TGF-β1 (0.5 ng/ml or 1 ng/mL) was combined with the IL-6, IL-8, MCP-1, and TIMP-1 cytokines, an additional 2-fold induction was found (bars 5 and 6, **Figure 2C**). It is important to note that the fold of induction by combining five cytokines was similar to that induced by the CM derived from 8505C and 16T cells (compare bars 5 and 6 with bars 7 and 9, **Figure 2C**). Interestingly, the combined treatment of THP-1 cells with IL-6, IL-8, MCP-1, TIMP-1, and TGF-β1 resulted in a higher expression of CD163 than what was found in CM derived from 11T cells (compare bars 5 and 6 with bar 8, **Figure 2C**). These data indicated that the combined cytokines of IL-6, IL-8, MCP-1, TIMP-1, and TGF-β1 could account for most of the induction activity found in CM derived from ATC cells. Taken together, these data show that these cytokines collaborate to facilitate the induction of M2 from THP-1 cells.

Activation of membrane receptor signaling pathways by the combined cytokines facilitates M2 induction

Activation of JAK/STAT, MEK/ERT, and PI3K/AKT has been reported to facilitate M2 polarization [14-17]. We therefore assessed the effects of the five cytokines on the activity of STAT3, MEK/ERK, and PI3K/AKT pathways to understand how these cytokines could collaborate to induce M2 (**Figure 3A**). While TGF-β1 had virtually no effect on the JAK2/STAT3 activity (**Figure 3B-I-a-d**; and **3B-II-a** and **3B-II-b**), the activity of JAK2/STAT3 was elevated by IL-6, IL-8, MCP-1, and TIMP-1 (**Figure 3B-I**, lanes 2 and 3; and **3B-II-a** and **3B-II-b**, bars 2 and 3). While TGF-β1 weakly suppressed the ERK activity, it was elevated by IL-6, IL-8, MCP-1, and TIMP-1 (**Figure 3B-I**, lanes 2 and 3; and **3B-II-c**, bars 2 and 3). IL-6, IL-8, MCP-1 and TIMP-1 had no apparent effects, whereas TGF-β1 activated PI3K/AKT/mTOR/p70 S6 signaling (**Figure 3B-I**; **3B-II-d-f**, bars 4 and 5). These data supported the notion that the combinatory effects of these cytokines could collaborate to activate the JAK2/STAT3, ERK and PI3K/AKT, signaling to facilitate the induction of M2.

We next evaluated the effects of CM derived from 8505C, 11T, and 16T cells on the activity of JAK2/STAT3, ERK, and PI3K/AKT pathways. We first showed that the major M2 marker, CD163, was expressed at the protein level when THP-1 cells were treated with CM from the three ATC cells (**Figure 3C-I-a**; and **3C-II-a**, bars 2, 3, and 4). Consistent with the findings from the effects of cytokines shown above, we found that the JAK2/STAT3 activity was increased by CM as evidenced by the elevated phosphorylated JAK2/STAT3 (**Figure 3C-I-b-e**; and **3C-II-b** and **3C-II-c**). The ERK activity was also elevated by CM derived from the three ATC cells (**Figure 3C-I-f** and **3C-I-g**; and **3C-II-d**). The activity of PI3K/AKT/mTOR/p70 S6 (**Figure 3C-I-h-m** and **3C-II-e-g**) was also increased by CM. All findings were normalized using β-actin as the control (**Figure 3C-I-n**). Therefore, the CM derived from 8505C, 11T, and 16T could

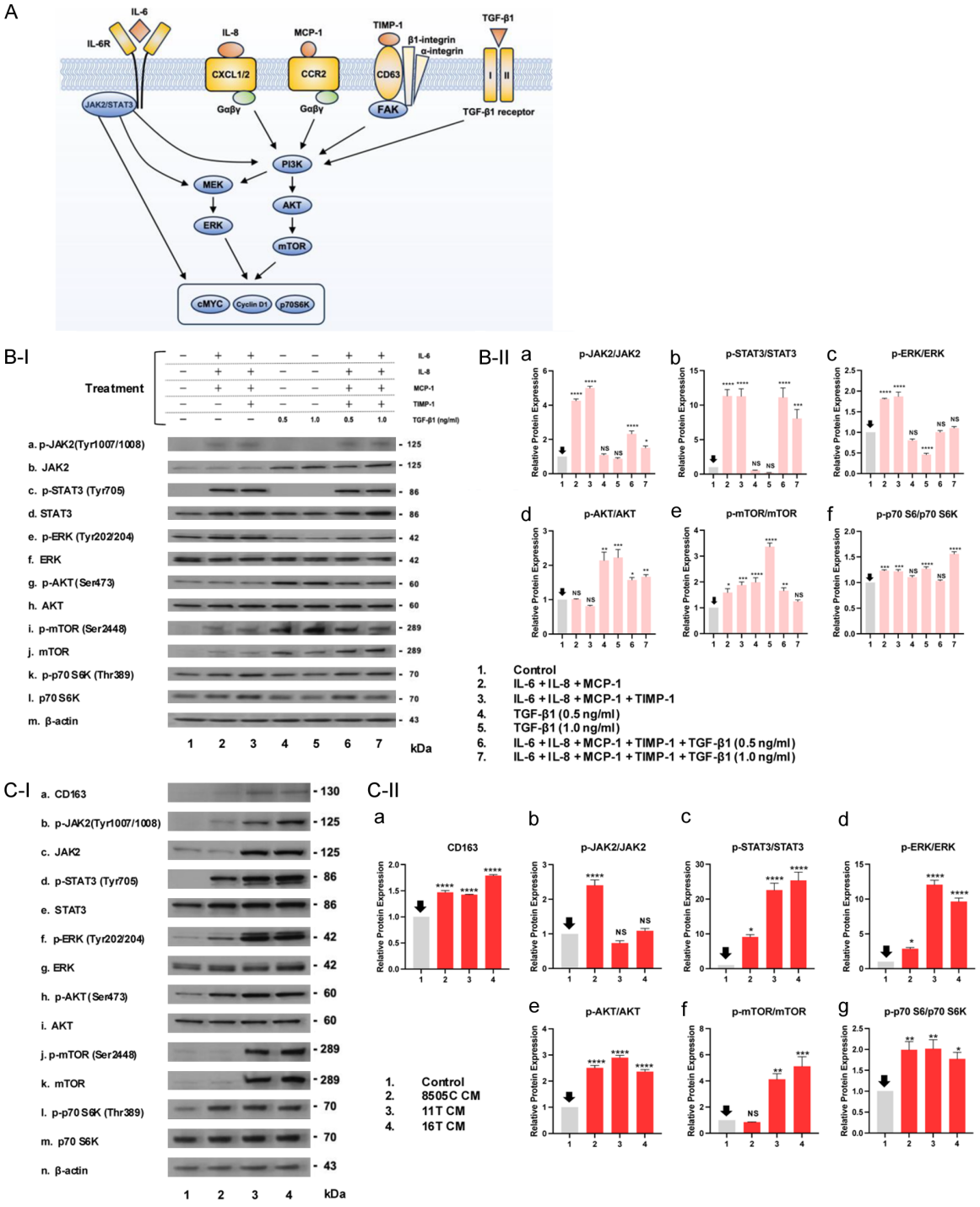

Figure 3. Activation of STAT3, ERK, and PI3K/AKT activity by combinatory actions of cytokines. A. Schematic diagram of signaling pathways activated by interaction of IL-6, IL-8, MCP-1, TIMP-1, and TGF-β1 with the membrane receptors. B. Representative Western blot analysis (B-I) and its quantitative analysis (B-II) show the effect of cytokines on the activity of the JAK2/STAT3 pathway and AKT/mTOR/p70 S6 pathway mediated by key effectors. THP-1 cells were treated with cytokines as shown (IL-6; 200 ng/ml, IL-8; 200 ng/ml, MCP-1; 10 ng/ml, TIMP-1; 100 ng/ml and TGF-β1; 0.5 or 1.0 ng/ml). C. Representative western blot analysis (C-I) and its quantitative analysis (C-II) showing the effect of CM derived from ATC 8505C, 11T, and 16T on the key effectors in the JAK2/STAT3, ERK, and PI3K/AKT/mTOR pathways. Data represent the mean ± SD (n=3). Significant differences are indicated by asterisks ($P < 0.05$ [*], $P < 0.01$ [**], $P < 0.001$ [***], and $P < 0.0001$ [****]). NS, not significant.

act to stimulate the JAK2/STAT3, ERK, and PI3K/AKT/mTOR/p70 S6 pathways similarly as by the five cytokines. These findings further supported that the combined five cytokines could facilitate the induction of M2.

Cross-interaction of M2-induced by CM with the ATC tumor cells

It is known that infiltrated TAMs can secrete growth factors to further drive the proliferation of tumor cells [18, 19]. We ascertained whether CM derived from ATC cells could lead to increased proliferation of cells by assessing Ki-67 levels by immune-staining. Compared with THP-1 cultured in the control media (**Figure 4A-I-a**), increased cell numbers were positive for Ki-67 when cultured in CM derived from 8505C (**Figure 4A-I-b**), 11T (**Figure 4A-I-c**) and 16T cells (**Figure 4A-I-d**). Quantitative analysis showed that cells positively stained with Ki-67 were increased by 21% more (**Figure 4A-II**). Furthermore, we found that the protein abundance of key proliferator markers, cMYC (**Figure 4B-I-a**, **4B-II-a**, **4B-I-c** as β-actin controls) and cyclin D1 (**Figure 4B-I-b**, **4B-II-b**), was elevated, indicating the stimulation of cell proliferation by CM derived from ATC.

To provide direct evidence that CM-induced M2 could potentially secrete factors to reciprocally stimulate proliferation of ATC tumor cells, we prepared green fluorescent protein (GFP)-labeled 8505C, 11T, and 16T cells. We then treated THP-1 cells with CM derived from 8505C, 11T, and 16T cells (**Figure 4C-I-b**) or with control regular media (**Figure 4C-I-a**), followed by co-culturing with GFP-labeled ATC cells and imaged by confocal imaging (**Figure 4C-II**). We found that the number of GFP-8505C co-cultured with THP-1 in CM (**Figure 4C-II-a**) was higher than in regular media (**Figure 4C-II-c**). While there were no apparent changes in the number of GFP-11T cells co-cultured with THP-1 in CM (**Figure 4C-II-e**) or in regular media (**Figure 4C-II-g**), GFP-16T was clearly higher in CM (**Figure 4C-II-i**) than co-culturing with THP-1 in regular media (**Figure 4C-II-k**). The increased cell numbers could be better visualized by the represented images shown in the insets (compare **Figure 4C-II-b** with **4C-II-d**, **4C-II-j** with **4C-II-i**). Quantitative analysis of the cell numbers indicated 1.3- and 1.9-fold increase of GFP-8505C and GFP-16T cells (**Figure 4C-III-a** and **4C-III-c**, respectively), co-culturing in CM than in regular media. It is of interest to note that proliferation of GFP-11T cells was not affected (**Figure 4C-III-b**). It is possible that the number of induced M2 cells by CM derived from 11T was not as high as those from 8505C and 16T cells. Nonetheless the data from 8505C and 16T cells supported the notion that CM-induced M2 could potentially secrete factors to reciprocally stimulate proliferation of ATC tumor cells, thereby further driving tumor cell progression.

Clinical relevance of cytokines identified in CM derived from human ATC

Our detailed molecular analysis has shown that the combined IL-6, IL-8, MCP-1, TIMP-1, and TGF-β1 facilitated the induction of M2 from THP-1 cells. An important question to be addressed is whether these cytokines play a critical role in the induction and infiltration of TAMs to TME that further propels human ATC progression. We therefore ascertained the clinical relevance of these five cytokines using a public human ATC database. Analysis of GSE33630 showed that the mRNA expression of *IL-6, IL-8*, *MCP-1*, *TIMP-1*, and *TGF-β1* was significantly increased in ATC than in normal subjects and papillary thyroid cancer (PTC) (**Figure 5A-I-a-e**). We further analyzed another dataset, GSE65144, which showed that except for *IL-6* and *MCP-1* (**Figure 5A-II-a** and **5A-II-c**, respectively), the mRNA expression of *IL-8, TIMP-1* and *TGF-β1* was significantly higher in ATC patients than the normal subjects (**Figure 5A-II-b**, **5A-II-d** and **5A-II-e**, respectively). This close association suggested that these cytokines could contribute to the induction of TAMs and further exacerbate ATC progression.

Discussion

The impact of TME on thyroid cancer progression has been documented [20, 21]. The extent of TAMs correlates with extrathyroidal extension and capsular invasion in DTC poorly [22]. Furthermore, human ATC was reported to have the greatest infiltration of TAMs in the TME, leading to poor survival rates [23].

These observations suggested that there are stimulatory cytokines secreted by ATC cells which could favor the infiltration and/or induction of M2. In this study, using THP-1 cells as a model, we identified common stimulatory

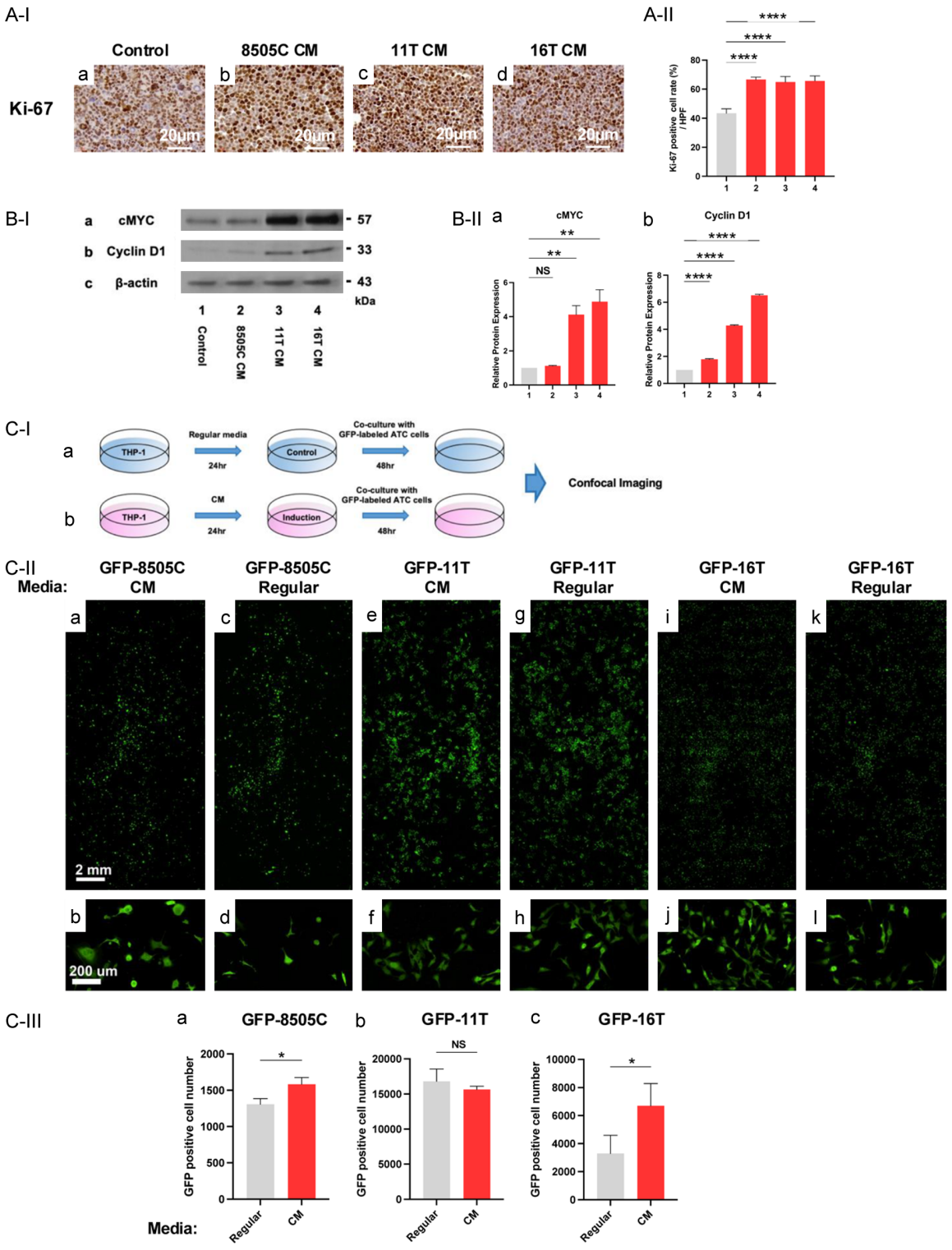

Figure 4. Cross-interaction of M2-induced by CM with ATC tumor cells. A. CM derived from 8505C, 11T, and 16T stimulated cell proliferation as shown by increased Ki-67 positively stained cells (A-I, representative micrographs of IHC; A-II, quantitation of Ki-67 positively stained cells) (magnification, bar scale =20 μm). B. Increased expression of cMYC and cyclin D1 in the protein levels in THP-1 cells treated by CM derived from ATC 8505C (lane 2), 11T (lane 3), and 16T cells (lane 4). Representative western blot analysis (B-I) and its quantitative analysis (B-II). C. Activated proliferation of GFP-ATC cells by the secreted growth factors from CM-induced M2. (C-I) Representative experimental scheme in the treatment of THP-1 cells cultured in control regular media (a), in CM media (b), followed

by co-culturing with GFP-labeled ATC cells. (C-II) Representative confocal images of green fluorescent cells were captured. Comparison of green fluorescent cells co-cultured in CM media (a, e and i) or in regular control media (c, g and k). Scale bar represents 2 mm in (a, c, e, g, i and k). (b, d, f, h, j and l) are zoomed insets from the respective images (a, c, e, g and i) (scale bar represents 200 μm in the inset images). (C-III) Quantitation of the cell numbers of GFP-8505C (a), GFP-11T (b), and GFP-16T cells (c). Data represent the mean ± SD (n=3). Significant differences are indicated by asterisks ($P < 0.05$ [*], $P < 0.01$ [**], $P < 0.001$ [***], and $P < 0.0001$ [****]). NS, not significant.

cytokines in the CM derived from the three ATC cell lines (**Figure 2A** and **2B**). Treatment of THP-1 with four cytokines (IL-6, IL-8, MCP-1, and TIMP-1) or singly with TGF-β1 only partially induced the expression of M2 marker CD163 (a read-out for M2 induction) (**Figure 2C** and Supplementary Figure 1) as compared with ATC cells derived-CM. Our results were consistent with those of previous studies that reported the participation of TGF-β1 in M2-like macrophage polarization. For instance, Zhang et al demonstrated that THP-1 cells treated with TGF-β were polarized into an M2-like phenotype [13]. Similarly, in a recent study, we showed that, like THP-1 cells treated with ATC cells derived-CM, monocytes incubated with TGF-β1 also exhibited a significant increase in the expression of classic M2 markers, including CD163 and Dectin-1. Moreover, inhibitors of the TGF-β receptor partially inhibited macrophage polarization induced by treatment with CM derived from 8505C [24]. Remarkably, when THP-1 cells were treated with the combination of five cytokines (IL-6, IL-8, MCP-1, TIMP-1, and TGF-β1), the extent of induction of M2 mimicked the full capacity of CM (see **Figure 2C**). Our results suggested that induction of M2 necessitated the collaboration of the activity of multiple cytokines. However, at present, we cannot exclude the contributions of other minor activators/cytokines present in the ATC-derived CM that could also participate in the induction of M2. Identification of other minor contributors would need to await further studies.

We elucidated how the five cytokines could collaborate to induce M2 by analyzing their effects on JAK/STAT, MEK/ERK, and PI3K/AKT pathways. The activation of these pathways has been shown to be involved in promoting M2 induction by five cytokines. IL-6 signaling is mediated by membrane-bound IL-6-specific receptor subunit (IL-6R)/signal-transducing gp130 receptor subunit, leading to the phosphorylation of the immediate effector, JAK/STAT, and downstream signaling (see **Figure 3A**). The activation of IL-6/JAK/STAT regulates cell proliferation, angiogenesis, and M2 polarization [25, 26]. Interestingly, we have previously found that ATC cells secreted IL-6 [27]. In addition, the incubation of human monocytes with ATC-cell-derived CM promoted the increase in the expression and secretion of IL-6 in these cells via the induction of STAT3 phosphorylation [6]. IL-6/JAK/STAT can also be involved in cross-signaling with MEK/ERK and PI3K/AKT pathways. The biological effects of IL-8 (CXCL8) are mediated by binding to its two membrane G protein-coupled receptors, CXCR1 and CXCR2. IL-8/receptor complexes activate AKT, MAPK, and PKC downstream signaling to affect immune functions, promoting growth and differentiation of monocytes-macrophages, proliferation, and angiogenesis [28]. Tissue inhibitor of metalloproteinases-1 (TIMP-1) is a naturally occurring inhibitor of metalloproteinases (MMPs) [29]. In addition, TIMP-1 acts as a signaling molecule with cytokine-like activities through PI3K/AKT and receptor-tyrosine kinase/RAS/RAS/MAPK signaling pathways [30] which are involved in M2 polarization [31]. The monocyte chemoattractant protein-1 (MCP-1/CCL2) is a member of the C-C chemokine family, and a potent chemotactic factor for monocytes [32]. MCP-1 acts in the recruitment of peripheral monocytes to inflammatory sites and tumors, and to promote M2 polarization of macrophages *in vitro* [33]. The biological activity of MCP-1 is mediated by the MCP-1/C-C motif chemokine receptor 2 (CCR2) axis, leading to the activation of PI3K/AKT, c-Raf/MEK/ERK, and MAPK pathways [34]. The signaling pathways of TGF-β1 contributes to the basic cellular processes through its interplay with JAK/STAT, MEK/ERK, and PI3K/AKT pathways [35]. The above reports suggested that analysis of the effects of five cytokines on the activity of JAK/STAT, MEK/ERK, and PI3K/AKT pathways could help us understand how these cytokines could collaborate for the induction of M2 in ATC. Indeed, we found that TGF-β1 acted to suppress ERK signaling, but greatly activated PI3K/AKT signaling, though TGF-β1 had no effects on the STAT3 activity. In agreement with these findings, we did not observe any significant changes in the phosphorylation of STAT3

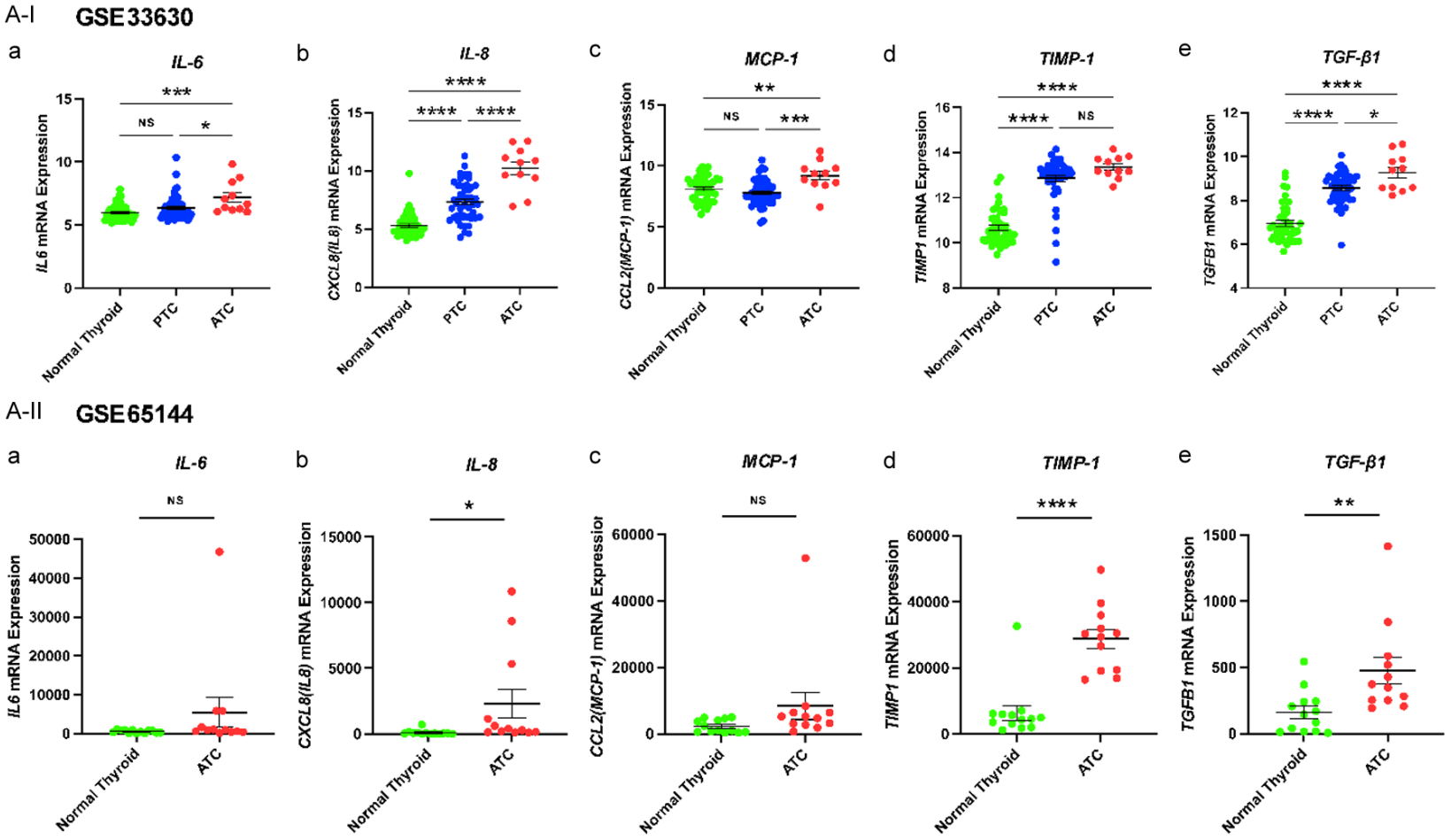

Figure 5. The mRNA expression of IL-6, IL-8, MCP-1, TIMP-1, and TGF-β1 is elevated in human ATC as compared with normal subjects and/or papillary thyroid cancer (PTC). Analysis using the Gene Expression Omnibus (GEO) database. (A-I) Data from GSE33630. Comparison of *IL-6*, *CXCL8*, *CCL2*, *TIMP-1*, and *TGF-β1* mRNA expression among normal subjects (n=45), PTC (n=49), and ATC (n=11). (A-II) Data from GSE65144. Comparison of *IL-6*, *CXCL8*, *CCL2*, *TIMP-1*, and *TGF-β1* mRNA expression among normal subjects (n=13) and ATC (n=12). Data represent the mean ± SD. Significant differences are indicated by asterisks ($P < 0.05$ [*], $P < 0.01$ [**], $P < 0.001$ [***], and $P < 0.0001$ [****]). NS, not significant.

in THP-1 cells treated with 20 ng/ml TGF-β1 [24]. The other four cytokines (IL-6, IL-8, MCP-1, and TIMP-1), though lacking the capacity to stimulate PI3K/AKT activity, exhibited stimulatory effect on the JAK/STAT3 and ERK signaling. These findings indicate that the five cytokines together can compensate for the insufficient capacity of a single cytokine in one pathway, leading to complete activity mediated by these signaling pathways, that are collectively needed for M2 induction. This conclusion is supported by the analysis of the effects of ATC-derived CM on the STAT3, ERK, and PI3K/AKT activity, in which the CM concurrently activated these three pathways (**Figure 3C**). However, at present, we cannot rule out the contributions of additional signaling pathways in the induction of THP-1 differentiation into M2-like macrophages by ATC cells. For instance, it has been demonstrated that the Notch signaling pathway, among others, also influences macrophage activation [36]. Whether this and other signaling pathways are involved in macrophage polarization and activation by ATC-derived CM will be investigated in future studies.

Recent studies have shown that TAMs could secrete growth factors to reciprocally promote tumor growth [37]. M2-induced by CM derived from ATC cells were reported to promote thyroid cancer cell migration and to decrease T cell proliferation [6]. In view of the findings that TAMs constitutes up to 50% of the TME in human ATC tumors [22], we therefore explored whether M2 induced from 8585C-, 11T- and 16T-CM could secrete stimulatory factors to drive tumor cell proliferation. Indeed, this stimulatory effect was shown by confocal imaging of GFP-labeled 8505C, 11T, and 16T cells (**Figure 4C**). The growth promoting effects were more prominent in 8505C and 16T cells. For 11T cells, we did not observe the reciprocal growth promoting effect. It is possible that the CM-induction of M2 for 11T was not as robust as for 8505C and 16T cells (**Figure 1B**), thereby resulting in fewer 11T CM-induced M2 to provide adequate growth factors to go above the detection sensitivity in our assays. The differential effects in the induction of M2 by CM derived from the three ATC cells could be due to the different genetic lesions in these three ATC cells lines. Regardless, our data have shown that tumor cells release stimulatory cytokines to induce M2, which in turn, reciprocally produces growth factors to drive proliferation of tumor cells. The clinical relevance of our findings was demonstrated by the results that elevated mRNA expression of the five cytokines was closely associated with aggressive human ATC. Furthermore, using a TCGA database, we also found that a high mRNA expression of *IL-6*, *MCP-1*, *IL-8* and *TGF-β1* was associated with decreased survival of PTC patients (Supplementary Figure 2). Taken together, the cytokines that we have identified could play an important role in M2 induction in the TME to drive ATC tumor cell growth.

Intensive efforts have been put forward to pursue immunotherapy for thyroid cancer, especially for ATC for which treatment options are very limited. TAMs is the major cell component of TME, which is known to play critical roles in ATC tumor genesis, progression, and metastasis. Thus, TAMs has been considered a potential therapeutic target. The present studies showed that induction of M2 required collaboration of multiple cytokines, suggesting that targeting TAMs by using monotherapy of inhibitors may not be effective to mitigate TAMs activity. Furthermore, the differential outcome of induction of M2 by CM from three ATC cell lines suggests that the genetic lesions will modulate the capacity of induction and infiltration of TAMs in the TME. Thus, targeting the TME in ATC could be a promising opportunity as well as a challenge for investigators in the coming years.

Acknowledgements

We are grateful to Dr. Chi-Ping Day from the Laboratory of Cancer Biology and Genetics, CCR, NCI for the LV-GFP-Luc virus used in the present study. We thank Ms. Swati Priya, Laboratory of Molecular Biology, CCR, NCI, for manuscript editing assistance. The work presented was supported by the Intramural Research Program of the NIH, National Cancer Institute, and Center for Cancer Research.

Disclosure of conflict of interest

None.

Address correspondence to: Dr. Sheue-Yann Cheng, Gene Regulation Section, Laboratory of Molecular Biology, National Cancer Institute, National Institutes of Health, 37 Convent Dr., Room 5128, Bethesda, MD 20892-4264, USA. Tel: 240-760-7828; Fax: 240-541-4498; E-mail: chengs@mail.nih.gov

References

[1] Li M, He L, Zhu J, Zhang P and Liang S. Targeting tumor-associated macrophages for cancer treatment. Cell Biosci 2022; 12: 85.

[2] Liu M, Liu L, Song Y, Li W and Xu L. Targeting macrophages: a novel treatment strategy in solid tumors. J Transl Med 2022; 20: 586.

[3] Zhu S, Yi M, Wu Y, Dong B and Wu K. Roles of tumor-associated macrophages in tumor progression: implications on therapeutic strategies. Exp Hematol Oncol 2021; 10: 60.

[4] Shin E and Koo JS. Cell component and function of tumor microenvironment in thyroid cancer. Int J Mol Sci 2022; 23: 12578.

[5] Marlow LA, D'Innocenzi J, Zhang Y, Rohl SD, Cooper SJ, Sebo T, Grant C, McIver B, Kasperbauer JL, Wadsworth JT, Casler JD, Kennedy PW, Highsmith WE, Clark O, Milosevic D, Netzel B, Cradic K, Arora S, Beaudry C, Grebe SK, Silverberg ML, Azorsa DO, Smallridge RC and Copland JA. Detailed molecular fingerprinting of four new anaplastic thyroid carcinoma cell lines and their use for verification of RhoB as a molecular therapeutic target. J Clin Endocrinol Metab 2010; 95: 5338-5347.

[6] Stempin CC, Geysels RC, Park S, Palacios LM, Volpini X, Motran CC, Acosta Rodriguez EV, Nicola JP, Cheng SY, Pellizas CG and Fozzatti L. Secreted factors by anaplastic thyroid cancer cells induce tumor-promoting M2-like macrophage polarization through a TIM3-dependent mechanism. Cancers (Basel) 2021; 13: 4821.

[7] Zhu X, Park S, Lee WK and Cheng SY. Potentiated anti-tumor effects of BETi by MEKi in anaplastic thyroid cancer. Endocr Relat Cancer 2019; 26: 739-750.

[8] Enomoto K, Zhu X, Park S, Zhao L, Zhu YJ, Willingham MC, Qi J, Copland JA, Meltzer P and Cheng SY. Targeting MYC as a therapeutic intervention for anaplastic thyroid cancer. J Clin Endocrinol Metab 2017; 102: 2268-2280.

[9] Zhu X, Zhao L, Park JW, Willingham MC and Cheng SY. Synergistic signaling of KRAS and thyroid hormone receptor beta mutants promotes undifferentiated thyroid cancer through MYC up-regulation. Neoplasia 2014; 16: 757-769.

[10] Kimura T, Doolittle WKL, Kruhlak M, Zhao L, Hwang E, Zhu X, Tang B, Wolcott KM and Cheng SY. Inhibition of MEK signaling attenuates cancer stem cell activity in anaplastic thyroid cancer. Thyroid 2024; 34: 484-495.

[11] Day CP, Carter J, Weaver Ohler Z, Bonomi C, El Meskini R, Martin P, Graff-Cherry C, Feigenbaum L, Tuting T, Van Dyke T, Hollingshead M and Merlino G. "Glowing head" mice: a genetic tool enabling reliable preclinical image-based evaluation of cancers in immunocompetent allografts. PLoS One 2014; 9: e109956.

[12] Pachitariu M and Stringer C. Cellpose 2.0: how to train your own model. Nat Methods 2022; 19: 1634-1641.

[13] Zhang F, Wang H, Wang X, Jiang G, Liu H, Zhang G, Wang H, Fang R, Bu X, Cai S and Du J. TGF-beta induces M2-like macrophage polarization via SNAIL-mediated suppression of a pro-inflammatory phenotype. Oncotarget 2016; 7: 52294-52306.

[14] Mao Y, Chen L, Wang F, Zhu D, Ge X, Hua D and Sun J. Cancer cell-expressed B7-H3 regulates the differentiation of tumor-associated macrophages in human colorectal carcinoma. Oncol Lett 2017; 14: 6177-6183.

[15] Zhao S, Mi Y, Guan B, Zheng B, Wei P, Gu Y, Zhang Z, Cai S, Xu Y, Li X, He X, Zhong X, Li G, Chen Z and Li D. Tumor-derived exosomal miR-934 induces macrophage M2 polarization to promote liver metastasis of colorectal cancer. J Hematol Oncol 2020; 13: 156.

[16] Jimenez-Garcia L, Higueras MA, Herranz S, Hernandez-Lopez M, Luque A, de Las Heras B and Hortelano S. A hispanolone-derived diterpenoid inhibits M2-Macrophage polarization in vitro via JAK/STAT and attenuates chitin induced inflammation in vivo. Biochem Pharmacol 2018; 154: 373-383.

[17] Cai J, Huang L, Tang H, Xu H, Wang L, Zheng M, Yu H and Liu H. Macrophage migration inhibitory factor of Thelazia callipaeda induces M2-like macrophage polarization through TLR4-mediated activation of the PI3K-Akt pathway. FASEB J 2021; 35: e21866.

[18] Caillou B, Talbot M, Weyemi U, Pioche-Durieu C, Al Ghuzlan A, Bidart JM, Chouaib S, Schlumberger M and Dupuy C. Tumor-associated macrophages (TAMs) form an interconnected cellular supportive network in anaplastic thyroid carcinoma. PLoS One 2011; 6: e22567.

[19] Xu Y, Wang X, Liu L, Wang J, Wu J and Sun C. Role of macrophages in tumor progression and therapy (Review). Int J Oncol 2022; 60: 57.

[20] Mirshahidi S, Yuan IJ, Simental A, Lee SC, Peterson NR, Andrade Filho PA, Murry T, Duerksen-Hughes P and Yuan X. Targeting tumor microenvironment akt signaling represents a potential therapeutic strategy for aggressive thyroid cancer. Int J Mol Sci 2023; 24: 5471.

[21] Han PZ, Ye WD, Yu PC, Tan LC, Shi X, Chen XF, He C, Hu JQ, Wei WJ, Lu ZW, Qu N, Wang Y, Ji QH, Ji DM and Wang YL. A distinct tumor microenvironment makes anaplastic thyroid cancer more lethal but immunotherapy sensitive than papillary thyroid cancer. JCI Insight 2024; 9: e173712.

[22] Ryder M, Ghossein RA, Ricarte-Filho JC, Knauf JA and Fagin JA. Increased density of tumor-

associated macrophages is associated with decreased survival in advanced thyroid cancer. Endocr Relat Cancer 2008; 15: 1069-1074.
[23] Jung KY, Cho SW, Kim YA, Kim D, Oh BC, Park DJ and Park YJ. Cancers with higher density of tumor-associated macrophages were associated with poor survival rates. J Pathol Transl Med 2015; 49: 318-324.
[24] Jaroszewski A, Geysels RC, Volpini X, Pellizas CG, Motran CC, Stempin CC, Nicola JP, Cheng SY and Fozzatti L. Anaplastic thyroid cancer cell-secreted TGFbeta1 plays a key role in inducing macrophage polarization of human monocytes. Am J Cancer Res 2024; 14: 3626-3638.
[25] Huang B, Lang X and Li X. The role of IL-6/JAK2/STAT3 signaling pathway in cancers. Front Oncol 2022; 12: 1023177.
[26] Ahmed I and Ismail N. M1 and M2 macrophages polarization via mTORC1 influences innate immunity and outcome of ehrlichia infection. J Cell Immunol 2020; 2: 108-115.
[27] Fozzatti L, Alamino VA, Park S, Giusiano L, Volpini X, Zhao L, Stempin CC, Donadio AC, Cheng SY and Pellizas CG. Interplay of fibroblasts with anaplastic tumor cells promotes follicular thyroid cancer progression. Sci Rep 2019; 9: 8028.
[28] Vilotic A, Nacka-Aleksic M, Pirkovic A, Bojic-Trbojevic Z, Dekanski D and Jovanovic Krivokuca M. IL-6 and IL-8: an overview of their roles in healthy and pathological pregnancies. Int J Mol Sci 2022; 23: 14574.
[29] Wu B, Arumugam S, Gao G, Lee GI, Semenchenko V, Huang W, Brew K and Van Doren SR. NMR structure of tissue inhibitor of metalloproteinases-1 implicates localized induced fit in recognition of matrix metalloproteinases. J Mol Biol 2000; 295: 257-268.
[30] Ries C. Cytokine functions of TIMP-1. Cell Mol Life Sci 2014; 71: 659-672.
[31] Zajac E, Schweighofer B, Kupriyanova TA, Juncker-Jensen A, Minder P, Quigley JP and Deryugina EI. Angiogenic capacity of M1- and M2-polarized macrophages is determined by the levels of TIMP-1 complexed with their secreted proMMP-9. Blood 2013; 122: 4054-4067.
[32] Yoshimura T. The chemokine MCP-1 (CCL2) in the host interaction with cancer: a foe or ally? Cell Mol Immunol 2018; 15: 335-345.
[33] Sierra-Filardi E, Nieto C, Dominguez-Soto A, Barroso R, Sanchez-Mateos P, Puig-Kroger A, Lopez-Bravo M, Joven J, Ardavin C, Rodriguez-Fernandez JL, Sanchez-Torres C, Mellado M and Corbi AL. CCL2 shapes macrophage polarization by GM-CSF and M-CSF: identification of CCL2/CCR2-dependent gene expression profile. J Immunol 2014; 192: 3858-3867.
[34] Wang L, Lan J, Tang J and Luo N. MCP-1 targeting: shutting off an engine for tumor development. Oncol Lett 2022; 23: 26.
[35] Gordeeva O. TGFbeta family signaling pathways in pluripotent and teratocarcinoma stem cells' fate decisions: balancing between self-renewal, differentiation, and cancer. Cells 2019; 8: 1500.
[36] Kerneur C, Cano CE and Olive D. Major pathways involved in macrophage polarization in cancer. Front Immunol 2022; 13: 1026954.
[37] Lv J, Liu C, Chen FK, Feng ZP, Jia L, Liu PJ, Yang ZX, Hou F and Deng ZY. M2-like tumour-associated macrophage-secreted IGF promotes thyroid cancer stemness and metastasis by activating the PI3K/AKT/mTOR pathway. Mol Med Rep 2021; 24: 604.

Supplementary Table 1. A list of antibodies in this study

Reagent	Source	Identifier	Dilusion
Mouse anti CD163	Santa Cruz Biotechnology, Dallas, TX, USA	Cat#sc-20066	1:250
Mouse anti β-actin	Santa Cruz Biotechnology	Cat#sc-47778	1:10000
Rabbit anti STAT3	Cell Signaling Technology, Danvers, MA, USA	Cat#4904S	1:2000
Rabbit anti Phospho-STAT3	Cell Signaling Technology	Cat#9145S	1:2000
Rabbit anti ERK	Cell Signaling Technology	Cat#9102S	1:1000
Rabbit anti Phospho-ERK	Cell Signaling Technology	Cat#9101S	1:1000
Rabbit anti AKT	Cell Signaling Technology	Cat#9272S	1:1000
Rabbit anti Phospho-AKT	Cell Signaling Technology	Cat#9271S	1:1000
Rabbit anti mTOR	Cell Signaling Technology	Cat#2972S	1:1000
Rabbit anti Phospho-mTOR	Cell Signaling Technology	Cat#2971S	1:1000
Rabbit anti p70 S6	Cell Signaling Technology	Cat#9202S	1:1000
Rabbit anti Phospho-p70 S6	Cell Signaling Technology	Cat#9205S	1:1000
Rabbit anti cMYC	Abcam, Cambridge Biomedical Campus, Cambridge, UK	Cat#ab32072	1:2000
Rabbit anti Cyclin D1	Abcam	Cat#ab16663	1:2000

Supplementary Table 2. Primer sequences used in this study

Gene name	Forward sequence	Reverse sequence
CD163	GAGACAGCGGCTTGCAGTT	TAGACACAGAAATTAGTTCAGCAGC
CD204	AGTGCTGCTTTCTTTAGGACGA	AGCTGTCATTGAGCGAGCAT
CCL13	GATCTCCTTGCAGAGGCTGAAG	TCTGGACCCACTTCTCCTTTGG
IL-10	AAGAAGGCATGCACAGCTCA	TGCAGCTGTTCTCAGACTGG
VEGFA	TAAGTCCTGGAGCGTTCCCT	ACGCGAGTCTGTGTTTTTGC
GAPDH	GGAGCGAGATCCCTCCAAAAT	GGCTGTTGTCATACTTCTCATGG

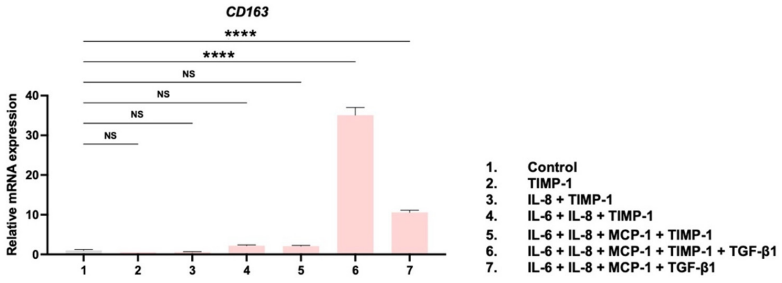

Supplementary Figure 1. RT-PCR result shows the effect for *CD163* expression by combined cytokine treatment (IL-6; 200 ng/ml, IL-8; 200 ng/ml, MCP-1; 10 ng/ml, TIMP-1; 100 ng/ml and TGF-β1; 20 ng/ml). Data represent the mean ± SD (n=3). Significant differences are indicated by asterisks ($P < 0.05$ [*], $P < 0.01$ [**], $P < 0.001$ [***], and $P < 0.0001$ [****]). NS, not signifcant.

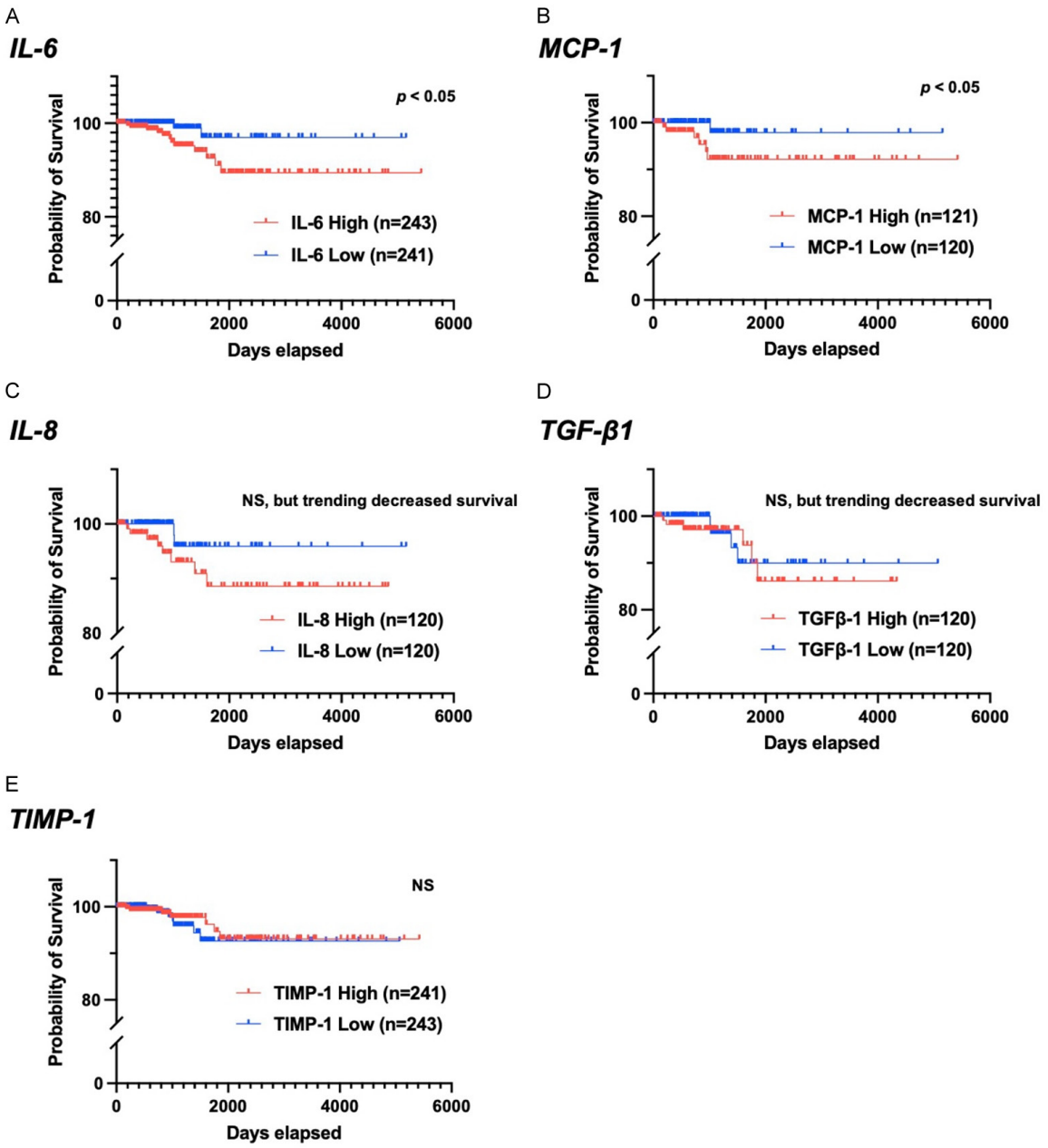

Supplementary Figure 2. Kaplan-Meier survival curves from TCGA, depicting the survival of papillary thyroid cancer patients according to the expression levels of cytokine-associated genes. A-E. Kaplan-Meier survival curves from TCGA-THCA datasets. A. IL-6; B. MCP-1; C. IL-8; D. TGF-β1; E. TIMP-1. NS, not significant.